

SSC18-VII-01

Engineering-Model Results of X-band Synthetic Aperture Radar for Small Satellite and Its Application to Constellation Mission

Hirobumi Saito,

Prilando Rizki Akbar, Kouji Tanaka, Makoto Mita,

Japan Aerospace Exploration Agency, Institute of Space and Astronautical Science
3-1-1, Yoshinodai, Chuo, Sagamihara, Kanagawa, 252-5210 Japan; 81-50-3362-2657
saito.hirobumi@jaxa.jp

Budhaditya Pyne, Tomoki Kaneko, Toshihiro Obata, Shinichi Nakasuka

The University of Tokyo

7-3-1, Hongo, Bukyo-ku Tokyo, 113-8656 Japan; 81-42-759-8104
Budhaditya.Pyne@ac.jaxa.jp

Jiro Hirokawa

Tokyo Institute of Technology

2-12-1-S3-19 O-okayama, Meguro-ku, Tokyo, 152-8522 Japan; 81-3-5734-2563
jiro@ee.e.titech.ac.jp

Seiko Shirasaka, Hiromi Watanabe, Kei-ichi Hirako

Keio University

4-1-1 Hiyoshi, Kohoku-ku, Yokohama, Kanagawa 223-8526 Japan; 81-45-564-2581
shirasaka@sdm.keio.ac.jp, h-watanabe@ac.jaxa.jp

Koichi Ijichi

Japan Space Systems

3-5-8 Shibakoen, Minato-ku, Tokyo 105-0011 Japan
Ijichi-Koichi@jspacesystems.or.jp

ABSTRACT

This paper presents the engineering model results of this X band synthetic aperture radar for small satellites and its application to constellation missions. The specifications of SAR performance are single polarization SAR with 1m ground resolution at 350 km altitude and with 3m ground resolution at 600km altitude orbit. A satellite is supposed to be 130kg in mass and the size is 0.7m x 0.8m x 0.9m on a rocket. A size of the deployed antenna is 4.9m x 0.7m. A chirped transmitting signal is amplified in a six GaN HEMT 200W amplifier modules to be combined in a waveguide resonator. The type of antenna system is deployable plane antenna due to its compact stow volume. Novel parallel plate slotted array antennas have been developed. We have performed compact range test, near-field measurement of an antenna wing with 2.8m x 0.7m size. The peak aperture efficiency is measured to be higher than 50%. We will launch the first demonstration satellite in late 2019. We finally will build a constellation of several tens SAR satellites with 1-3m resolution to realize from every day to every few hours revisit.

1 INTRODUCTION

Synthetic Aperture Radar (SAR) is a well-known remote sensing technique [1,2] with reliable capabilities. Large or medium size satellites with hundreds kilograms or more can afford SAR sensors. Medium SAR satellites such as SAR-Lupe[1] (Germany, total mass 770kg, 2006), TecSAR[4] (Israel, 300kg, 2008), and NovaSAR-S[3] (United Kingdom, 400kg) have been launched. ASNARO-2 (Japan, 500kg) is planned to be launched. These large or medium satellites cost hundreds million US dollars including launching cost.

In this paper, we describe a synthetic aperture radar sensor compatible with 100kg class satellites. When

this small SAR satellite is injected to typical earth observation orbit with 500-600km altitude, its ground resolution is expected to be 3-10m that is useful for earth observation and monitoring. If this satellite is injected to a low earth orbit with 300km altitude, the ground resolution can be 1m although life time of the satellite is short.

Section 2 discusses on a SAR system scaling law and the specification of a SAR system that is compatible with 100 kg class small satellite. Section 3 describes the technology developments and test results of the engineering model. Section 4 and 5 are for future plane and conclusion.

2 SIZING of SAR SYSTEM

In order to realize a SAR system that is compatible with a small satellite, a SAR scaling law should be considered, paying attention to satellite resources (RF power and antenna size), and SAR performances (resolution and image quality). The details are described in [4-6].

$$\sigma_{NE} \circ \delta_r = (8\pi R^3 k T_o v_{st}) (NFL_s) \frac{\lambda}{P_{TX-ave} A^2 \eta^2} \quad (1)$$

where σ_{NE} (a noise equivalent sigma zero) is a radar cross section per unit area for which signal-to-noise ratio is unity. This value is widely used as an index of SAR image quality. δ_r is a ground range resolution, R is a distance between the satellite and the observation target, k is the Boltzmann constant, $T_o=290K$, v_{st} is a satellite velocity, NF is a noise figure of the receiving system, L_s is a system loss, P_{TX-ave} is an average transmitting RF power, λ is an observation wavelength. A and η are an area and an aperture efficiency of the antenna.

The left-hand side of Eq.(1) is a performance index, namely a product of its ground resolution and the image noise. The right-hand side corresponds to the resources required to realize its performance such as a RF power, an antenna area, a noise figure, and RF loss. Note that the required resource term is inversely proportional to an average RF power and a square of antenna area and is proportional to an observation wavelength. A RF power and antenna area required to obtain a constant SAR performance $\sigma_{NE} \circ \delta_r$ (resolution times noise) become smaller as observation wavelength is shorter. If we accept a coarse ground resolution, then the image quality can be improved.

We have designed a X band SAR compatible with 100kg class satellite as shown in Table 1. The RF peak power is selected to 1000 W that is realized by GaN solid state amplifiers, instead of vacuum tube TWTAs.

For a better image quality with $\sigma_{NE} = -20$ dB, a ground resolution of 10 m can be achieved. Furthermore a ground resolution of 3 m is realized if one accepts image degradation of $\sigma_{NE} = -15$ dB, which is still enough for sight recognition.

Another version of small SAR satellites is high resolution SAR with low altitude orbit. A ground

Table 1. Specification of SAR System Compatible with 100kg Class Satellite

Item	SAR Mode	
	Strip Map	Sliding Spot Light
Altitude	600km	300km
Resolution	3m	1m
Center Frequency	9.65GHz	
Swath	25 km	10 km
Chirp Band Width	75MHz	300MHz
Polarization	V/V	
Antenna Size	4.9 m×0.7 m	
Ant Panel Efficiency	50%	
TX Peak Power	1000~1100 W	
TX Duty	25%	
System Loss	3.5 dB	
System Noise Figure	4.3 dB	
Off Nadir Angle	15~45 deg	
Pulse Repetition Frequency	3000 ~ 8000 (TBD) Hz	
NESZ (beam center)	-15dB	-22dB
Ambiguity (beam center)	>15dB	

resolution of 1m can be obtained where the orbit altitude 300km, RF bandwidth 300MHz, and RF peak power 1000W. This orbit has only a short life and is limited to on-demand, responsive missions for disaster management.

We design 5minutes SAR observation in one earth revolution, paying attention to thermal design, power and data managements.

The SAR system is provided with a nominal strip-map mode and a spot-light mode with satellite attitude maneuver. There are two resolution modes. One is a fine resolution (3 meter) mode with degraded image quality ($\sigma_{NE} = -15$ dB) for sight-recognition application. Another is a coarse resolution (10 meter) mode with better image quality ($\sigma_{NE} = -20$ dB).

3 TECHNOLOGIES for SMALL SAR

3.1 Configuration of small SAR satellite

When we determine configuration of SAR system for small satellites, architecture of SAR antenna and RF feeding system is a critical issue. In general SAR system requires an antenna with several m² area. There have been several types of SAR antennas : 0) body mount antenna on a large satellite structure with 3-5m length (TerrSAR-X[7], Nova SAR-S[3]), 1a) deployable (passive) parabolic antenna with 3-4m diameter (SAR-Lupe[1], TecSAR[2], ASNARO-2), 1b) deployable passive plane antenna (Seasat[8], ERS-1[9]), 2a) deployable active phased array with centralized TX/RX module (RadarSat-1[10]), 2b) deployable active phased array antenna with distributed TX/RX modules (ALOS 1, 2[11], RadarSAT-2[12]). Table 2 shows architectures of deployable SAR antenna and feeding

system, excluding 0) body mount antenna.

The types of body mount antenna 0) and parabola antenna 1a) are not applicable for small satellites that require small stowed size. In the case 2a) and 2b) the active phased array antennas with phase shifters or TX/RX modules are exposed to harsh space environments. Complicated design and manufacturing processes with thermal, structure, and RF issues are required and drastic cost-down seems impossible.

Possible configuration of a 100Kg SAR satellite compatible piggy back launch is satellite outlook shown in Fig.1. All electric instruments are installed in the satellite body and several passive antenna panels are deployed to compose antenna area of several m². Its

Table 2 Architecture of SAR antenna and Feeding System for Small SAR

	deployable Passive Antenna		deployable Active Phased Array Antenna	
	1a) Parabola	1b) Passive Plane Antenna	2a) Centralized TX/RX	2b) Distirbuted TX/RX
Examples	TecSAT, ASNARO2	Seasat-A, ERS-1, MicroXSAR	RadarSAT-1	RadarSAT-2,ALOS-1,2
Characteristics	X large stowed size X mechanical complexity △ medium cost X no scan mode	○ compact stowed size possible ○ no instruments on panel ○ low cost X no scan mode	X medium stowed size △ instruments on panel △ medium cost ○ scan mode	X large stowed size X instruments on panel X high cost ○ scan mode
system				

LNA: low noise amplifier
HPA: high power amplifier

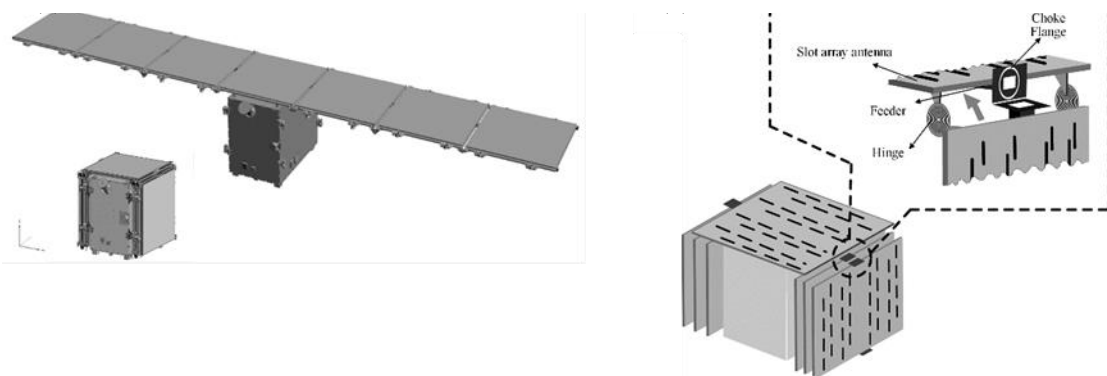


Fig.1 (Left) Outlook of small SAR satellite. 0.7x 0.7 x 0.7m³ in stowed configuration. Antenna size is 4.9m x 0.7m. (Right) Non-contact waveguide feeding with choke flange at hinge.

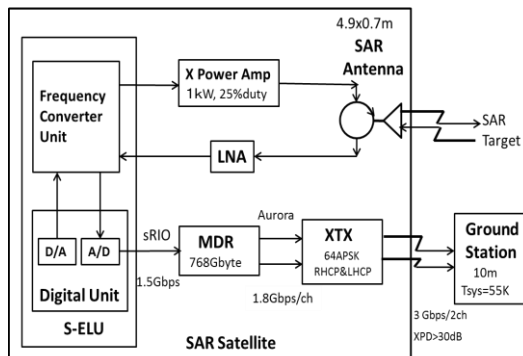


Fig.2 System block diagram of small SAR
MDR: Mission data Recorder,
XTX: band Transmitter
S-ELU: SAR – Electronics Unit

stowed size is 0.7m x0.7m x0.7m and the solar cells are installed at the rear side of the antenna. Figure 1 shows the conceptual configuration of our small SAR antenna.

Then we can proceed to design system block of small SAR. All electronics instruments are in a satellite body. Figure 2 is a system block diagram of small SAR system. The details are described in the following sections. Note that electrical power is generated by flexible solar cells installed on the back side of SAR antenna.

3.2 Deployable plane antenna

As shown in Table 1, the SAR system requires an antenna of several meters in orbit. A stowed size of the satellite in a rocket should be less than $0.7 \times 0.7 \times 0.7 \text{m}^3$ for small launchers. One of the most feasible candidates is passive, deployable, honeycomb panel antenna with slot array [13, 14]. This antenna is friendly with a plane honeycomb structure and relatively high aperture efficiency.

Figure 3 shows structure of an antenna panel. Its size is about 70cm x 70cm x 0.6cm. The waveguide is embedded at the center of the rear surface in order to feed RF to the antenna panel through coupling slots. The antenna panel consists of a dielectric honeycomb core and metal skins, which work as a parallel plate guide for RF. The front surface with two dimensional array of radiation slots works as an antenna radiator for vertical polarization SAR mode. In order to achieve 1m ground resolution, the antenna bandwidth should be about 300MHz. This antenna is a traveling wave array antenna. Therefore, length of an array branch should be less than about 30cm.

In order to make antenna instrumentation simpler, TX and RX instruments are in the satellite body. Therefore

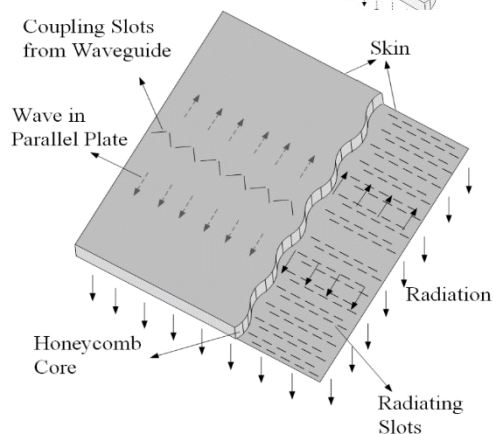
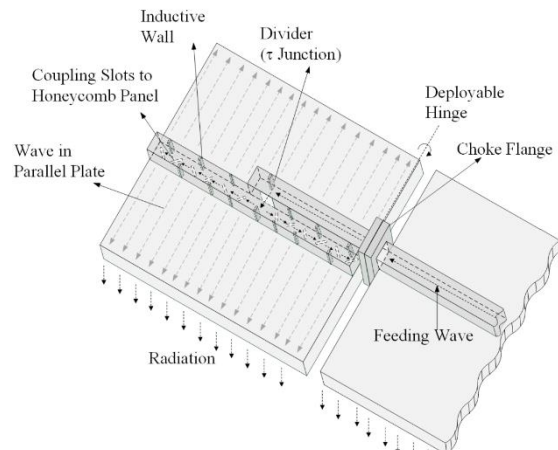


Fig.3 Structure of antenna panel. Upper part is outlook with feeding waveguide. In lower part feeding waveguide is omitted to explain antenna function.

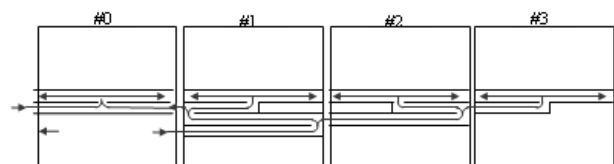


Fig.4 Waveguide feeder network is embedded in antenna panels. Panel #0 is on satellite body. Left wing is symmetric and omitted in this figure.

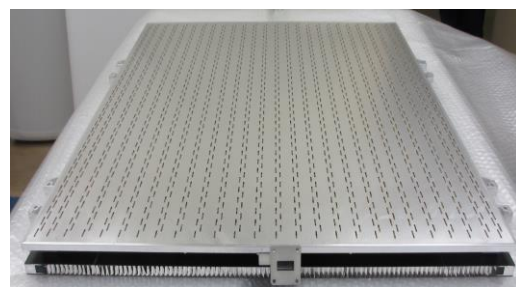


Fig.5 Photograph of engineering model of antenna panel #3. 70cmx70cm.

RF should be fed from the satellite body to each panel with equal electric length. Figure 4 is the waveguide feeding networks for an antenna wing. Panel #0 is on the satellite body and the other wing is symmetric configuration. Figure 5 is the photograph of the engineering model of antenna panel #3 (70cmx70cm).

3.3 RF Feeder with non-contacting waveguide flange

The next problem is to feed RF to each antenna panel at the deployable hinges. There are conventional RF feeding methods to deployable antenna such as flexible cables, flexible waveguides and rotary joints. However, they have disadvantages of large RF loss, resistive torque and structural complexity.

We apply choke flanges of waveguides to this problem in order to realize RF feeding with non-contacting waveguide flanges [15]. Choke flanges have been widely used to avoid the degradation of current conduction through waveguide flanges due to manufacturing imperfections or oxidization of the flange surfaces. There is a ditch whose depth and distance from a wide wall of a waveguide are roughly a quarter of the wavelength λ . The ditch works as a quarter-wave resonance short-circuit stub. Although there is a gap at the main waveguide, wall current flows smoothly with low impedance at the gap.

Each antenna panel with a feeder waveguide is connected by a deployment hinge. After deployment, a choke and a cover flange face to each other. RF loss can be minimized by the choke connection even though there is a physical gap between two waveguide flanges.

We have measured the effect of choke flanges. For a newly developed choke, RF loss is below 0.05dB at all regions of our frequency band and the possible misalignment. Note that reflection at the gap is less than -25dB.

3.4 Engineering model of one antenna wing

We are developing electrical model, structural model and engineering model of one antenna wing which consists of four panels with size of 2.8m x0.7m. Figure 6 is a photograph of near field RF measurement and photogrammetry measurement of engineering model at A-Metlab Facility, Kyoto University. Figure 7 shows the antenna directivity of several panel configurations such as single panel (#3), two-panels (#2+#3), three-panels (#1+#2+#3) and four-panels (#0+#1+#2+#3). The panel identification number is indicated in Fig.3. The peak directivities at the center frequency 9.65GHz are 36.7dBi for one-panel, 39.6dBi for two-panels, 41.6dBi for three-panels, and 42.4dBi for four-panels, respectively. These values are almost proportional to number of the panels in decibel,

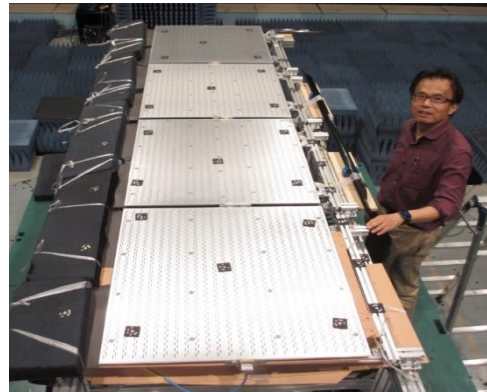


Fig.6 Near field RF measurement and photogrammetry measurement of engineering model (one wing, four panels, 2.8m x0.7m) at A-Metlab Facility, Kyoto University.

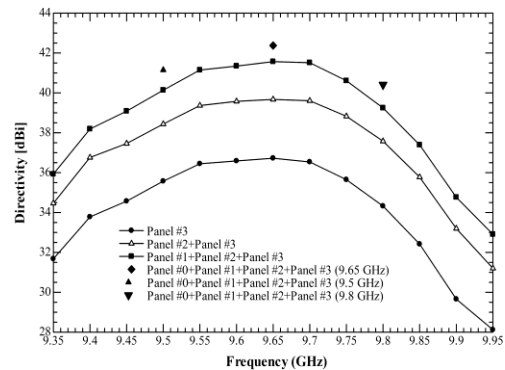


Fig.7 Antenna directivity as function of frequency by near field measurement. Antenna configurations are single panel, two-panels, three-panels and four-panels (2.8mx0.7m).

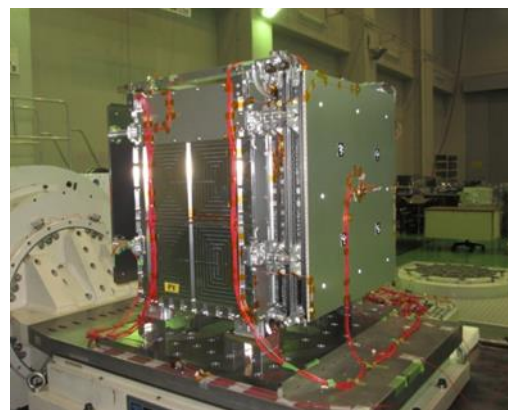


Fig.8 Structure model vibration test of antenna wing stowed on satellite body.

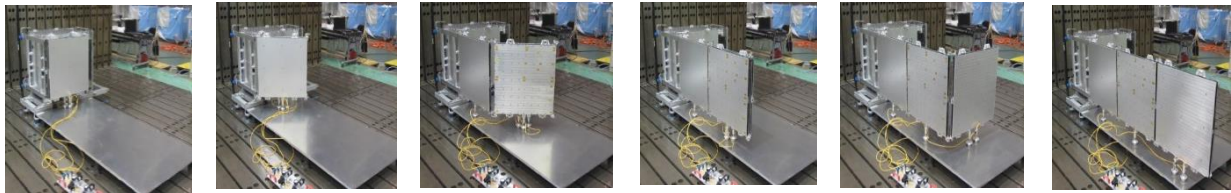


Fig.9 Deployment test of one-wing antenna structural model with air bearing system. We measure surface shape after deployment by photogrammetry measurement.

indicating that effective in-phase excitation of antenna panels is achieved and antenna arraying can work as designed.

Figure 8 is a photograph of structure model vibration test of antenna wing stowed on satellite body. We also performed deployment tests of one wing antenna model with air bearing system. The surface shape after deployment is measured by photogrammetry measurement to confirm the antenna surface accuracy. Figure 9 is a photograph of the deployment test. The stow-deployment configuration is “wrapped-round” type, the merit of which is that the hinge mechanical parts do not stick out from the radiation surfaces.

3.5 X band power amplifier

Recently advanced solid state amplifiers with GaN HEMT devices have been developed. They can replace a conventional, bulky TWTA that also requires high voltage power supply. At present we apply internal matching, 200 W pulse amplifier packages to our system[16]. Duty cycle ratio is also important for SAR performance (see Eq.(1)). Conventional SAR satellites have adopted duty cycle ratio of typically 10%. Our GaN amplifier modules are provided with higher duty cycle ratio of 25%, paying attention to its thermal design. The final amplifier stage of each amplifier module consists of two 200W rated-power devices in parallel, where one device amplifies 100W, half of rated-power output. In this case the device junction temperature is below 150 C and the device package temperature is below 90 C and the device reliability condition is satisfied. Two 100W outputs are combined in the micro-strip circuit to achieve 200W output. Then outputs of 6 amplifier modules are combined with a waveguide resonator combiner and obtain 1000W peak output [17].

The power amplifier modules and the power combiner are integrated directly on the satellite panel of aluminum alloy with 5kg mass. At operation of 1000W RF output, and duty cycle 25%, 1100W heat is generated at the amplifier system. This heat is stored at

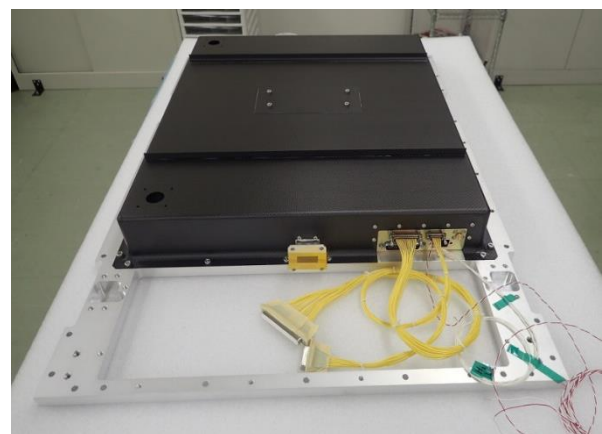


Fig.10 Photograph of X band Power Amplifier (XPA) on aluminum satellite panel.

the aluminum alloy panel and the temperature of panel increase by 50 degree after 5 minutes SAR operation. Then in about 50 minute the stored heat is irradiated to deep space from heat radiator surface of the panels. We confirmed this thermal design in thermo-vacuum test. Figure 10 is a photograph of X band Power amplifier (XPA).

3.6 SAR data processing and storage

A SAR-Electronics Unit (S-ELU) handles transmitting signal generation, receiving signal processing (frequency conversion and analog-to-digital conversion) for SAR sensor. The S-ELU for small satellites is being developed based on an airborne SAR instrument. The chirp bandwidth is 300MHz for 1m ground resolution. The received signal is converted to digital signal of 8bit x 720M sample/sec. Data compression rate is about 50%. Receiving duty cycle is about 50% to acquire timing with reasonable signal-to-noise ratio. The average data rate is 1.5Gbit/sec. In the SAR observation mode, this 1.5Gbit/sec SAR data is transferred to Mission Data Recorder (MDR) through serial RapidIO (sRIO) interface.

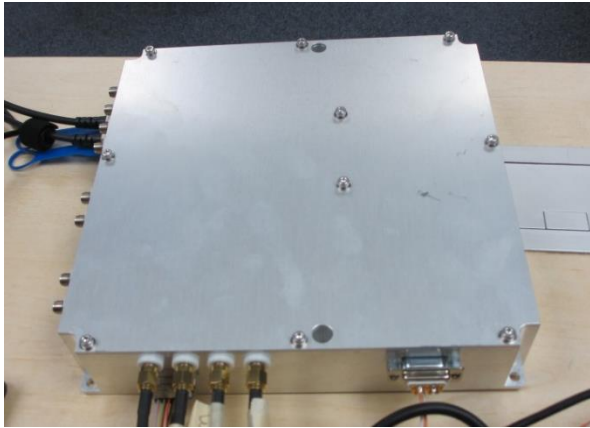


Fig.11 Photograph of Mission Data Recorder (MDR)

MDR consists of commercial 16 NAND flash memory devices and the total memory capacity is 768Gbyte. Total dose tolerance of NAND devices is confirmed by Co60 irradiation test. Single event upset errors are corrected by standard error correction code for commercial NAND devices. A commercial Xilinx UltraScale FPGA (Field Programmable Gate Array) device is utilized for high speed data flow and standard powerful error correction code. Special cares are paid to thermal heat path and thermal stress of BGA (Ball Brid Array) packaging. In down link communication mode, stored data is transferred to high data rate X band transmitter (XTX). XTX has dual polarization (RHCP/LHCP) channels to increase its down link capability. Stored data is switched to the 2 channels and they are transferred to XTX through Xilinx Aurora data interface. The data rate between MDR and XTX is 2Gbit/sec per one channel and total data rate is 4Gbit/sec. Figure11 is a photograph of Mission Data Recorder (MDR).

3.7 SAR data down link to ground station

The observed data is transmitted to ground station through high-speed X band link. We have already demonstrated high speed downlink of 64 APSK, 100Msps with Hodoyoshi 4 satellite in 2014[18]. Based on this technology, we are developing dual polarization channel X band link with total 2-3Gbit/sec capability[19]. Allocated radio frequency for earth observation is 8025-8400MHz (375MHz bandwidth). However, next band 8400-8450MHz is deep space down link band that should be protected against possible interference. We select 64APSK modulation with 300Msymbol/sec to observe the protection regulation. We apply DVB-S2X standard to this high speed down link.

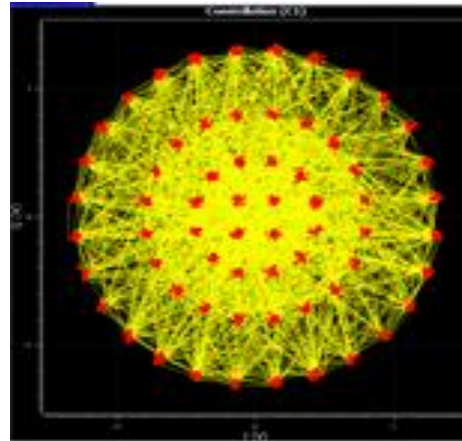


Fig.12 Demodulated constellation of 64APSK, DVB-S2X format, 1.45Gbps/ch.

Digital processing of the transmitting signal including DVB-S2X standard formatting, I-Q mapping, route Nyquist filtering is performed by a commercial Xilinx UltraScale FPGA. A commercial, high-performance digital-to-analog converter is applied to generate 1.2 GHz IF signal. Special cares are also paid to thermal heat path and thermal stress of BGA (Ball Brid Array) packaging. This IF signal is frequency up-converted to X band and is amplified up to 1W at RF section. Nonlinearity, especially third-order intermodulation, of the final power amplifier is critical issue of the RF section. Figure12 is demodulated constellation pattern of 64APSK, DVBS-2X, 1.45Gbps/channel. Error vector magnitude is about -27dB rms.

In order to secure the dual polarization channel link, Cross Polarization Discrimination (XPD) factor is important for communication link system to avoid interference between dual channels. Dominant factors are XPD of atmosphere propagation and XPD of onboard and ground antenna. We have developed the corrugated horn antenna and the septum polarizer for this purpose. The antenna gain is 17dBi and XPD is higher than 33dB.

A ground receiving antenna with 10m diameter is being developed. Existing 10m antenna for Ku band at JAXA, Usuda is converted to X band receiving antenna. The antenna gain, system noise temperature, and XPD is 56.5dBi, 55K (zenith), and >35dB, respectively.

Received RF signals at the ground station are frequency down converted and are stored at a dual channel, high speed, and large volume data recorder. Non-real time software demodulation system is being developed.

This high speed down link system is demonstrated by the first Minisatellite of “Innovative Satellite Technology Demonstration Program” and is planned to

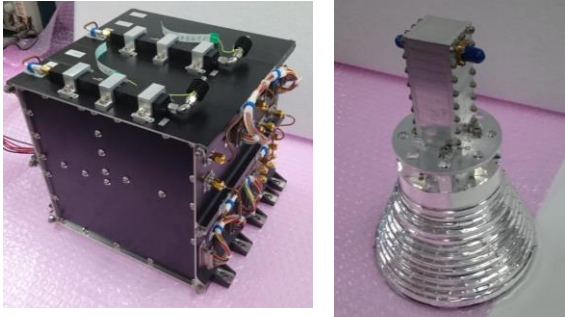


**Fig.13 Left:High speed X band Transmitter(XTX)
Right : Medium Gain Antenn (MGA)**

be launched in 2019. Figure13 is a photograph of flight model of high speed X band Transmitter (XTX) and Medium Gain antenna (MGA).

4. FUTURE RLANE

A company, Synspective, is established in this year. The company plans to develop a small SAR satellite to demonstrate this small SAR system. The launch is scheduled in late 2019. Also we are developing 3kW power amplifiers to realize 1m ground resolution. Then the company will construct a constellation of small SAR satellites with 1m ground resolution. The rapid information from the SAR constellation will be processed and be provided to customers.

5 CONCLUSION

This paper describes the system and the engineering model test of a X band SAR which is compatible to a 100kg class satellite. When this small SAR satellite is injected to typical earth observation orbit with 500-600 km altitude, its ground resolution is expected to be 3-10m that is useful for earth observation and monitoring. If this satellite is injected to a low earth orbit with 300km altitude, the ground resolution can be 1m. The first demonstration is plane in 2019.

6. ACKNOWLEDGEMENT

This research was funded by ImPACT Program of Council for Science, Technology and Innovation (Cabinet Office, Government of Japan).

7. REFERENCES

[1] H. M. Braun, P. E. Knobloch, "SAR on Small Satellites- Shown on the SAR-Lupe Example" ,

Proceedings of the International Radar Symposium 2007 (IRS 2007), Cologne, Germany, Sept. 5-7, 2007.

[2] U. Naftaly and R. Levy - Nathansohn, "Overview of the TECSAR satellite hard- ware and mosaic mode," IEEE Geoscience and Remote Sensing Letters, vol.5, no. 3, pp.423-426, 2008.

[3] Philip Davies, Phil Whittaker, Rachel Bird, Luis Gomes, Ben Stern, Prof Sir Martin Sweeting, Martin Cohen, David Hall, "NovaSAR-S Bringing Radar Capability to the Disaster Monitoring Constellation" 4S Symposium, Slovenia, June 2012.

[4] M.I Skolnik, "Radar Handbook Third Edition," McGraw-Hill, USA, 2008.

[5] K. Tomiyasu, "Tutorial review of synthetic-aperture radar (SAR) with applications to imaging of the ocean surface," Proc. of The IEEE, vol.66, no.5, pp. 563-583, May 1978.

[6] H. Saito, et. al., "Synthetic aperture radar compatible with 100kg class piggy-back satellite," IEEE, APSAR2013(2013 Asia-pacific conference on synthetic aperture radar), TU2.R1.4, 2013.

[7] B. Grafmuller, A. Herschlein, and C. Fischer, "The Terra SAR-X antenna system," in IEEE International Radar Conference, 2005. Institute of Electrical & Electronics Engineers (IEEE), 2005. [Online]. Available: <http://dx.doi.org/10.1109/RADAR.2005.1435823>

[8] R. Jordan, "The Seasat-A synthetic aperture radar system," IEEE Journal of Oceanic Engineering, vol.5, no.2, pp.154 - 164, apr1980. [Online]. Available: <http://dx.doi.org/10.1109/JOE.1980.1145451>

[9] E. Attema, "The active microwave instrument onboard the ERS-1 satellite," Proceedings of the IEEE, vol.79, no.6, pp.791-799, jun1991. [Online]. Available: <http://dx.doi.org/10.1109/5.90158>

[10] R. Raney, A. Luscombe, E. Langham, and S. Ahmed, "RADARSAT (SAR imaging)," Proceedings of the IEEE, vol.79, no.6, pp.839-849, jun1991. [Online]. Available: <http://dx.doi.org/10.1109/5.90162>

[11] Y. Kankaku, Y. Osawa, S. Suzuki, and T. Watanabe, "The overview of the 1-band sar onboard alos-2," in Proceedings of Progress in Electromagnetics Research Symposium, 2009.

[12] S. Riendeau and C. Grenier, "RADARSAT - 2 antenna," in Aerospace Conference, 2007 IEEE. IEEE, 2007, pp.1-9.

[13] J. Hirokawa, et al, "Waveguide-fed parallel plate slot array antenna," IEEE Trans. antenna & propagation, vol.40, no.2, pp.218-222, Feb. 1992.

[14] Prilando Rizki Akbar, et al, " Parallel-plate slot array antenna for deployable SAR antenna onboard small satellite," IEEE Trans. antenna &

propagation, vol.64, no.5, pp.1661-1671, May,2016

- [15] H.Saito and A.Tomiki, : in progress for Japanese patent, 2013-128851.
- [16] H.Watanabe et al “1000W X-Band Microwave GaN Solid State Power Amplifier for Small SAR Satellite,” Small Satellites Systems and Services – The 4S Symposium 2018, paper 147, Sorrento, Italy. 28 May – 1 June.
- [17] V.Ravindra, H.Saito, J.Hirokawa, M.Zhang, and A.Tomiki, “A TM010 cavity power combiner with microstrip line inputs,” IEICE Trans. Electron., Vol.E100-C,No12, pp.1087-1096, Dec.2017
- [18] H. Saito, et. al., “High spectral-efficiency communications in X band for small earth-observation satellites - results of 505 Mbps demonstration and plan for 2 Gbps link -,” 4S Symposium 2016, Valletta, Malta, 30 May – 6 June, 2016.
- [19] T. Kaneko, et. Al., “2Gbps Downlink System of 100kg Class Satellite for Compact Synthetic Aperture Radar Mission ” , Small Satellites Systems and Services – The 4S Symposium 2018, paper 48, Sorrento, Italy. 28 May – 1 June.